Article

# Hydrogen Bonds-Enabled Design of a *C*-Symmetric Chiral Brønsted Acid Catalyst

Norie Momiyama, Kosuke Funayama, Hirofumi Noda, Masahiro Yamanaka, Naohiko Akasaka, Shintaro Ishida, Takeaki Iwamoto, and Masahiro Terada

*ACS Catal.*, **Just Accepted Manuscript** • DOI: 10.1021/acscatal.5b02079 • Publication Date (Web): 21 Dec 2015

# Hydrogen Bonds-Enabled Design of a $C_1$-Symmetric Chiral Brønsted Acid Catalyst

Norie Momiyama,*[,†] Kosuke Funayama,[‡,§] Hirofumi Noda,[¶] Masahiro Yamanaka,[¶] Naohiko Akasaka,[‡] Shintaro Ishida,[‡] Takeaki Iwamoto,[‡] and Masahiro Terada*[,‡,⊥]

[†]Institute for Molecular Science, and SOKENDAI (The Graduate School for Advanced Studies), Okazaki, Aichi 444-8787, Japan

[‡]Department of Chemistry, Graduate School of Science, Tohoku University, Aoba-ku, Sendai 980-8578, Japan

[§]Graduate Research on Cooperative Education Program of IMS with Tohoku University

[¶]Department of Chemistry, Faculty of Science, Rikkyo University, Toshima-ku, Tokyo, 171-8501, Japan

[⊥]Analytical Center for Giant Molecules, Graduate School of Science, Tohoku University, Aoba-ku, Sendai 980-8578, Japan

**ABSTRACT:** We have developed new $C_1$-symmetric, chiral bis-phosphoric acids with an electron-withdrawing group as one of the two substituents. This $C_1$-symmetric, chiral bis-phosphoric acid with a pentafluorophenyl group performs exceptionally well in the asymmetric Diels–Alder reaction of acrolein, methacrolein, and α-haloacroleins with substituted amidodienes. Control over the atropisomeric catalyst structure, enhancement of the catalytic activity, and differentiation of the asymmetric reaction space is possible by the remote control of the pentafluorophenyl group. Furthermore, we have conducted theoretical studies to clarify the roles of both intra- and intermolecular hydrogen bonds in the $C_1$-symmetric chiral environment of chiral bis-phosphoric acid catalysts. The developed strategy, $C_1$-symmetric catalyst design through hydrogen bonding, is potentially applicable to the development of other chiral Brønsted acid catalysts.

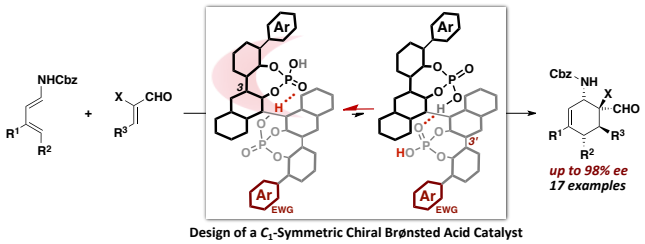


Design of a $C_1$-Symmetric Chiral Brønsted Acid Catalyst

**KEYWORDS:** *asymmetric catalysis, chiral Brønsted acid, cycloaddition, enantioselectivity, organocatalysis*

## INTRODUCTION

Asymmetric catalysis has been an active field of research since the early 1980s,[1] and the design of chiral ligands and chiral molecules has been recognized as one of the most valuable strategies. Therefore, a great deal of effort has been dedicated to this task.[2] On the other hand, design strategies for chiral catalysts have not changed much over the past two decades. Typically, conformationally rigid and $C_2$- or pseudo $C_2$-symmetry are elements used in catalyst design; for example, the axially chiral binaphthyl frameworks, which is a representative source of chirality.[3] Modification of this class of framework has proved fruitful and has greatly expanded the variety of catalytic asymmetric reactions that can be performed with a wide range of substrates and in a highly enantioselective fashion.

We previously developed the (*R*)-3,3'-di(2-hydroxy-3-arylphenyl)binaphthol-derived $C_2$-symmetric chiral bis-phosphoric acid ($C_2$-BISPA) catalyst, **1a** (Ar: 2,4,6-triisopropylphenyl (TRIP)), which efficiently catalyzes the enantioselective Diels–Alder reaction of α-H or α-alkylated acroleins with amidodienes (Eq 1, Figure 1).[4,5] An inherently atropisomeric, conformationally flexible naphthyl—phenyl framework has been successfully used as a new chiral component in the design of a chiral Brønsted acid catalyst.[6–9] X-ray diffraction analysis of $C_2$-BISPA **1b**, which possesses a phenyl group, indicates the existence of an intramolecular hydrogen bond between the two phosphoric acid moieties responsible for the creation of a $C_1$-symmetric, chiral environment (Figure 1(b) and 1(c)),[4a] in which high chiral efficiency and reasonable catalytic activity have been attained. Therefore, to establish strategies for the molecular design of chiral Brønsted acid catalysts with conformationally flexible frameworks, an understanding of how the hydrogen bond creates the $C_1$-symmetric chiral environment and how this controls the asymmetric reactions is especially important.[10] However, no detailed studies on either the intra- or intermolecular hydrogen bonding in these catalysts have been made. Herein, we describe our development of a new $C_1$-symmetric, chiral bis-phosphoric acid ($C_1$-BISPA), **2**, that possesses an electron-withdrawing group at the $C_{Naph}(3')—C_{Ar}(3)$ position to clarify the role of both intra- and intermolecular hydrogen bonding in

catalysis (Figure 2).[11] Moreover, the present study also establishes a new strategy to elaborate the asymmetric reaction space through hydrogen bonding directed by the remote control of the electron-withdrawing substituent.

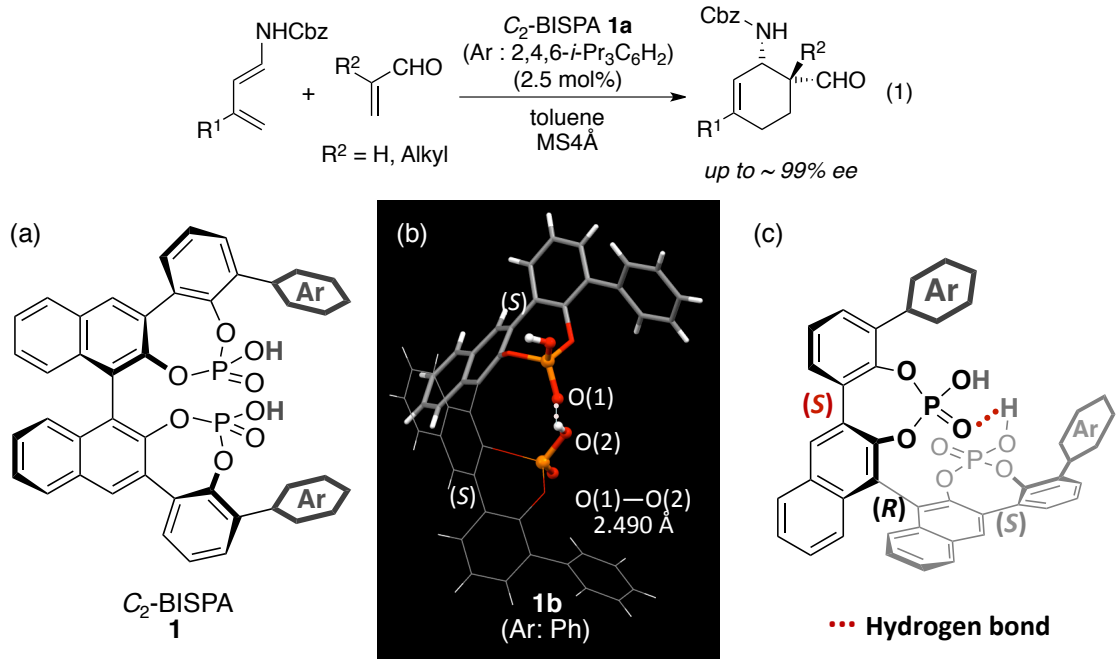


**Figure 1.** From a previous study on the $C_2$-symmetric bis-phosphoric acid ($C_2$-BISPA) **1**. (a) General chemical structure of $C_2$-BISPA **1**. (b) X-ray diffraction analysis of $C_2$-BISPA **1b** (Ar: Ph). Pink dashed line indicates the hydrogen bond. O(1)—O(2) = 2.490 Å. (c) Schematic structure of $C_2$-BISPA **1** indicating the hydrogen bond with red dashed line.

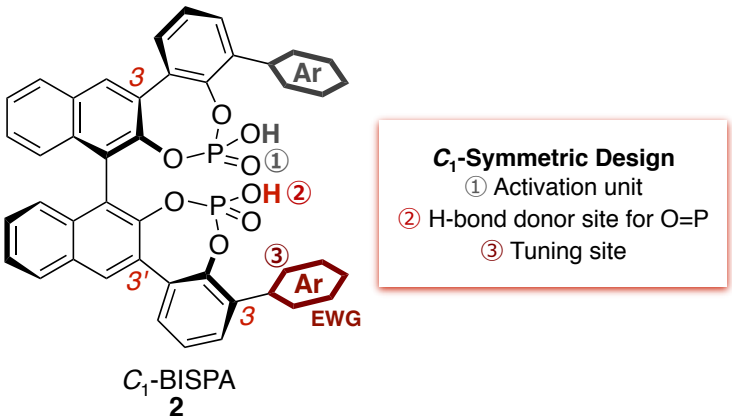


**Figure 2.** From this study: $C_1$-symmetric design of the chiral Brønsted acid, $C_1$-BISPA **2**, catalyst.

## RESULTS AND DISCUSSION

**Structural Requirements for Design of $C_1$-Symmetric Bis-Phosphoric Acid ($C_1$-BISPA) 2.** The hydrogen-bonding interaction was considered to play two roles in enantioselective Diels–Alder reaction of acroleins with amidodienes:[4a] controlling the atropo diastereomeric behavior derived from the naphthyl—phenyl axis, and activating an acrolein and a diene to facilitate enantioselective product formation. To apply the hydrogen-bonding interaction for $C_1$-symmetric catalyst design, we initially attempted to clarify the requirements of each catalyst component in detail.

We assembled $C_1$-BISPA **2a** and $C_1$-symmetric mono-phosphoric acids **3a** and **3b** to evaluate the importance of two phosphoric acid moieties in the catalytic enantioselective Diels–Alder reactions of α-haloacroleins[12] with *N*-Cbz amidodiene,[13] considering the synthetic versatility of the resulting adducts and, in addition, the advancement of this methodology (Table 1).[14–16] Treatment of α-bromoacrolein (**5a**) (1.5 equiv) with *N*-Cbz amidodiene **4a** (1.0 equiv) in toluene in the presence of 2.5 mol% of **2a** at –78 °C for 24 h resulted in the formation of **6aa** in 29% yield with 71% ee (1*S*,6*S*) (entry 1). In sharp contrast, the enantioselectivities in the presence of 5 mol% of **3a** or **3b** dropped significantly (8% ee) under the same conditions (entries 2 and 3). To gain supportive evidence of the importance of the hydrogen bond to improve the chemical and optical yields, we prepared $C_1$-BISPA **2b**. This catalyst possesses a bis-trifluoromethylphenyl substituent as an electron-withdrawing group at the $C_{Naph}(3')—C_{Ar}(3)$ position. We found, as hoped, that the chemical yield and the enantioselectivity improved to 65% yield and 85% ee (1*S*,6*S*), respectively, in the reaction catalyzed by **2b** (entry 4).

**Table 1.** Enantioselective Diels–Alder Reaction of α-Bromoacrolein (**5a**) with *N*-Cbz Amidodiene **4a**.[a]

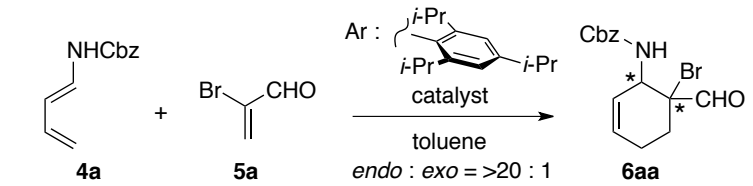


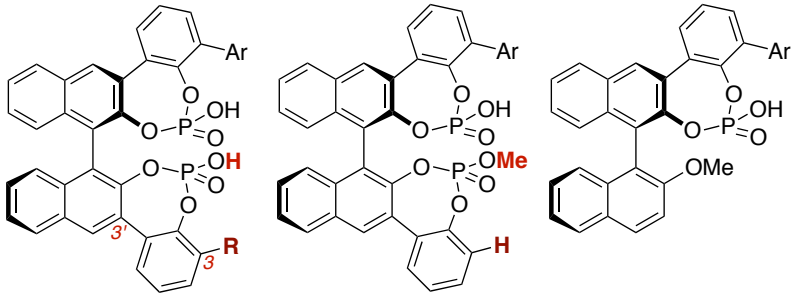


**2a** : R = H
**2b** : R = 3,5-$(CF_3)_2C_6H_3$

**3a** **3b**

| entry | catalyst | (mol%) | yield (%)[b] | ee (%)[c] | |
|---|---|---|---|---|---|
| 1 | **2a** | (2.5) | 29 | 71 | (1*S*,6*S*) |
| 2 | **3a** | (5.0) | 51 | 8 | (1*R*,6*R*) |
| 3 | **3b** | (5.0) | 50 | 8 | (1*S*,6*S*) |
| 4 | **2b** | (2.5) | 65 | 85 | (1*S*,6*S*) |

[a] Reactions were conducted with 1.0 equiv of **4a** and 1.5 equiv of **5a** in the presence of 2.5 mol% **2** or 5.0 mol% **3** in toluene at –78 °C. [b] Isolated yield. [c] Determined by chiral HPLC.

To give further insight into the structural differences and the enantioselectivities, we attempted to obtain crystal structures to verify their 3D structures. X-ray diffraction analysis revealed a diastereomeric mixture of **3b**. No obvious intra- or intermolecular hydrogen bonds were found, based on the distance between the oxygen atoms in the phosphoryl and methoxy groups.[17] In contrast, a single atropo diastereomer (*S*,*R*,*S*) of $C_1$-BISPA **2b** was obtained among the four possible atropo diastereomers: (*S*,*R*,*S*), (*S*,*R*,*R*), (*R*,*R*,*R*), and (*R*,*R*,*S*) (Figure 3).[18] Notably, although the atropo diastereomer (*S*,*R*,*S*) of **2b** is the same as those of $C_2$-BISPA catalysts **1a** and **1b**, two kinds of intramolecular hydrogen bonds were inferred based on the distance of the two oxygen atoms: -O(3)H—O(2)=P: 2.467 Å and -O(2')H—O(3')=P: 2.464 Å, indicating that both phosphoric acids, O(2)=P-O(1)H and O(3')=P-O(4')H, may function as activation units for the acroleins and amidodienes in $C_1$-BISPA **2**.

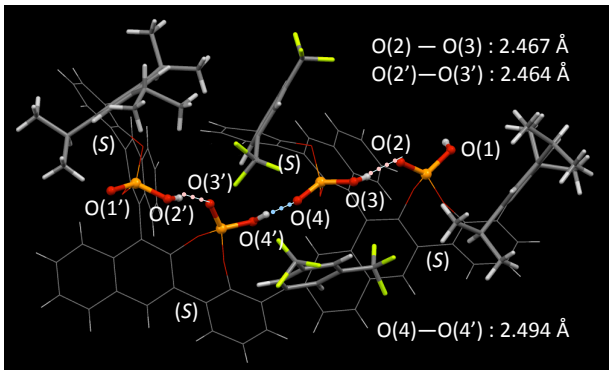


**Figure 3.** X-ray diffraction analysis of **2b**. Intramolecular distance between the two oxygen atoms (O(2)—O(3) = 2.467 Å, O(2')—O(3') = 2.464 Å, intramolecular hydrogen bonds are indicated by dashed pink line.) and intermolecular distance of two oxygen atoms (O(4)—O(4') = 2.494 Å, intermolecualar hydrogen bond is indicated by dashed light blue line.).

Combining the results of initial experiments and X-ray diffraction analyses, we inferred that the two phosphoric acid moieties and the presence of hydrogen bonding are primarily responsible for asymmetric induction, i.e., controlling the atropisomerism of the naphthyl—phenyl framework and transferring the axial chirality of binaphthyl to produce the enantiomerically enriched product. On the other hand, to be highly enantioselective, the reaction should proceed at the side of the sterically bulky TRIP substituent in $C_1$-BISPA **2** (Figure 4).

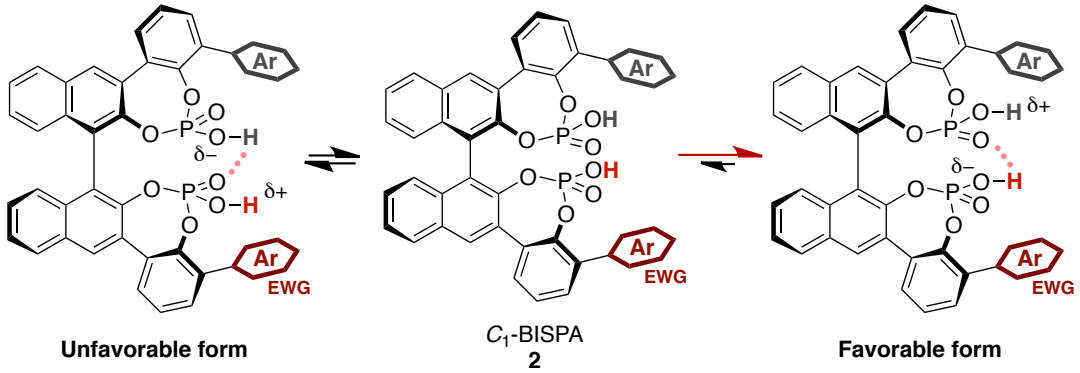


**Figure 4**. Two possible intramolecular hydrogen bondings and reaction spaces in $C_1$-BISPA **2**.

The $C_1$-symmetric catalyst design discussed above provides a powerful strategy if the following criteria can be satisfied; i.e., (i) the stereodynamic behavior of two

atropisomeric naphthyl—phenyl axes can be controlled by intramolecular hydrogen bond between the two phosphoric acids, (ii) they have the requisite catalytic activity by using the influence of the electron-withdrawing group, while keeping the sterically demanding TRIP group fixed as one of two substituents, and, (iii) of the two asymmetric reaction spaces, the asymmetric reaction take place on the side of the sterically demanding TRIP substituent at the $C_{Naph}(3)—C_{Ar}(3)$ position by the electron-withdrawing group. To further develop this strategy, we studied the details of the molecular design of $C_1$-BISPA modified with an electron-withdrawing group.

**Development of $C_1$-BISPA 2-catalyzed Enantioselective Diels–Alder Reaction of Substituted Acroleins 5 with *N*-Cbz Amidodienes 4.** The ability of $C_1$-BISPA **2b** was initially evaluated for a variety of α-haloacroleins **5** in the catalytic enantioselective Diels–Alder reaction with *N*-Cbz amidodiene **4a**. The preliminary experiments showed that $C_1$-BISPA **2b** can be used for the Diels–Alder reactions of α-chloroacrolein (**5b**) and α-iodoacrolein (**5c**).[19] For instance, in the case of α-chloroacrolein (**5b**), while the yield was not sufficient, the enantioselectivity of the Diels–Alder adduct **6ab** was high (38% yield, 90% ee after 24 h and 45% yield, 90% ee after 48 h). Therefore, we next focused on exploring the use of an electron-withdrawing group at the $C_{Naph}(3')—C_{Ar}(3)$ position to improve the product yield (Table 2). The reaction of **5b** with **4a** catalyzed by $C_1$-BISPA **2c**, which has a 3,4,5-trifluorophenyl group, produced a higher yield than that of $C_1$-BISPA **2b** (entries 1 and 2). We also confirmed that the pentafluorophenyl substitution of $C_1$-BISPA catalysts **2d** and **2e** improved not only the product yields but also the enantioselectivities (entries 3 and 4). For this reaction, the optimal quantities were found to be 1 equiv of **5b** with 2 equiv of **4a**, yielding the *endo* adduct **6ab** in the highest yield with higher enantioselectivity (entry 5).

We postulated that the acidity of one phosphoric acid proton near the TRIP substituent at the $C_{Naph}(3)—C_{Ar}(3)$ position is enhanced, and, at the same time, the asymmetric reaction space is controlled by the electron-withdrawing substituent at the $C_{Naph}(3')—C_{Ar}(3)$ and $C_{Naph}(3')—C_{Ar}(5)$ positions through intramolecular hydrogen bonding between the phosphoric acid proton and phosphoryl oxygen ($-OH_{EWG}\cdots O{=}P_{TRIP}$).[20] Consequently, the improved catalytic activity and the strongly directed hydrogen bond would improve the chemical and optical yields.

Finally, the corresponding reactions catalyzed by $C_2$-BISPA catalysts **1a**, **1c**, and **1d**

were conducted to assess the roles of both the steric- and electronic substituents (entries 6–8). $C_2$-BISPA **1a** produced a comparable yield and enantioselectivity to $C_1$-BISPA **2d** (entry 3 vs. 6). In sharp contrast, $C_2$-BISPA catalysts **1c** and **1d** were inferior to that of $C_1$-BISPA **2d** (entry 3 vs. 7 and 8), demonstrating the importance of the $C_1$-symmetric design and the steric- and electronic substituents. Moreover, these results suggested that the highly enantioselective reaction catalyzed by $C_1$-BISPA **2d** occurred around the asymmetric reaction space near the TRIP group, not near the electron-withdrawing group.

**Table 2.** Effect of the Electron-withdrawing Group of $C_1$-BISPA **2**, and a Comparison of **2** with $C_2$-BISPA **1** in the Enantioselective Diels–Alder Reaction of α-Chloroacrolein (**5b**) with *N*-Cbz Amidodiene **4a**.[a]

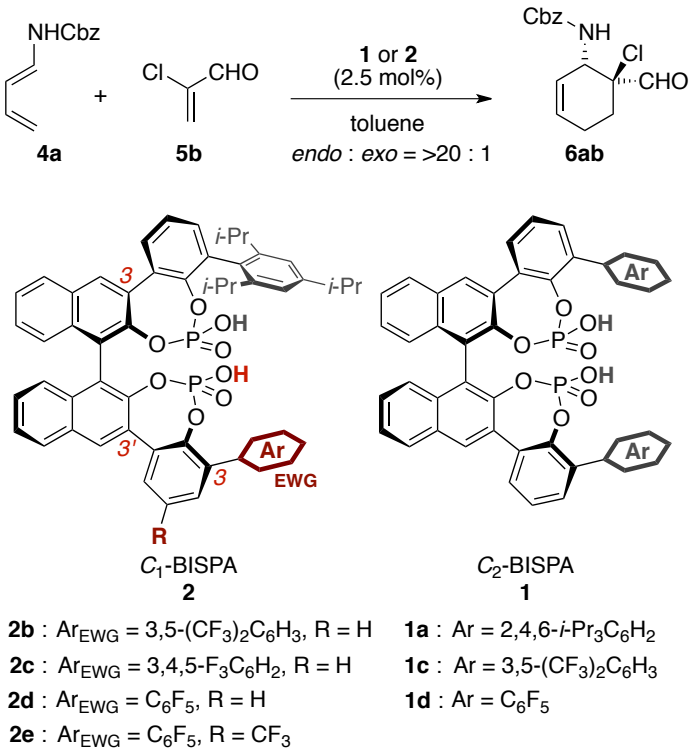


**2b** : $Ar_{EWG}$ = 3,5-$(CF_3)_2C_6H_3$, R = H
**2c** : $Ar_{EWG}$ = 3,4,5-$F_3C_6H_2$, R = H
**2d** : $Ar_{EWG}$ = $C_6F_5$, R = H
**2e** : $Ar_{EWG}$ = $C_6F_5$, R = $CF_3$

**1a** : Ar = 2,4,6-*i*-$Pr_3C_6H_2$
**1c** : Ar = 3,5-$(CF_3)_2C_6H_3$
**1d** : Ar = $C_6F_5$

| entry | catalyst | yield (%)[b] | ee (%)[c] |
|---|---|---|---|
| 1 | **2b** | 38 | 90 (1*S*,6*S*) |
| 2 | **2c** | 47 | 92 (1*S*,6*S*) |
| 3 | **2d** | 67 | 98 (1*S*,6*S*) |
| 4 | **2e** | 74 | 97 (1*S*,6*S*) |

| | | | | |
|---|---|---|---|---|
| 5[d] | **2d** | 98 | 97 | (1*S*,6*S*) |
| 6 | **1a** | 61 | 93 | (1*S*,6*S*) |
| 7 | **1c** | 30 | 5 | (1*S*,6*S*) |
| 8 | **1d** | 25 | 14 | (1*R*,6*R*) |

[a] Reactions were conducted with 1.0 equiv of **4a** and 1.5 equiv of **5b** in the presence of 2.5 mol% catalyst in toluene at –60 °C. [b] Isolated yield. [c] Determined by chiral HPLC. [d] Reactions were conducted with 2.0 equiv of **4a** and 1.0 equiv of **5b**.

With the rationally designed $C_1$-BISPA **2d** in hand, we turned our attention to testing its performance for substrate generality in the catalytic enantioselective Diels–Alder reaction of acroleins **5** with substituted amidodienes **4**. As can be seen in Table 3, the reactions were highly enantioselective for a range of acroleins and substituted amidodienes. The reactions to produce the corresponding cyclohexyl β-amino aldehydes (**6)** with high enantiofacial control proceeded smoothly for α-bromoacrolein (**5a**), α-chloroacrolein (**5b**), α-iodoacrolein (**5c**), acrolein (**5d**), and methacrolein (**5e**) (entries 2–5). Use of 3- or 3,4-disubstituted amidodienes **4** allows facile enantioselective access to substituted cyclohexyl β-amino aldehydes **6** (entries 6–16). In particular, 3,4-disubstituted amidodienes **4e**–**4i** substrates can be used (entries 11–16). Moreover, the first example of the catalytic enantioselective elaboration of 6-formyl-cyclo-2-hexcene-5-methyl (**6af**), which is a key intermediate in the synthesis of pumiliotoxin C reported by Overman,[21] can be carried out using the present method; however, the yield was low (entry 17).

**Table 3.** Enantioselective Diels–Alder Reaction of Acroleins **5** with Substituted Amidodienes **4**[a]

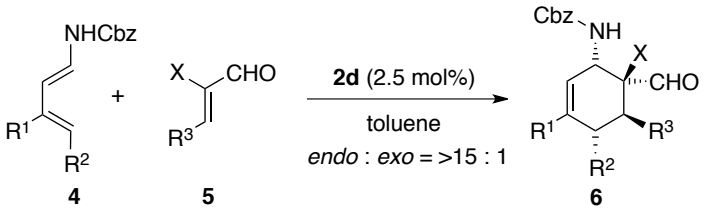

| entry | | 6 | yield (%)[b] | ee (%)[c] |
|---|---|---|---|---|
| 1 | 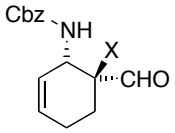 | X = Br (**6aa**) | 95 | 97 |
| 2 | | X = Cl (**6ab**) | 98 | 97 |
| 3[d] | | X = I (**6ac**) | 90 | 96 |
| 4[e] | | X = H (**6ad**) | 67 | 98 |
| 5 | | X = Me (**6ae**) | 99 | 96 |
| 6[d] | 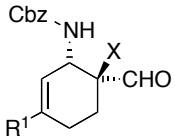 | $R^1$ = Me, X = Br (**6ba**) | 98 | 96 |
| 7[d] | | $R^1$ = Me, X = Cl (**6bb**) | 85 | 95 |
| 8[d] | | $R^1$ = Me, X = I (**6bc**) | 98 | 97 |
| 9[d] | | $R^1$ = Et, X = Br (**6ca**) | 98 | 96 |
| 10[d] | | $R^1$ = Bn, X = Br (**6da**) | 77 | 88 |
| 11[d] | 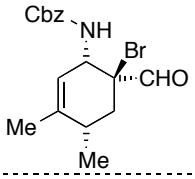 | (**6ea**) | 83 | 93 |
| 12[f,g] | 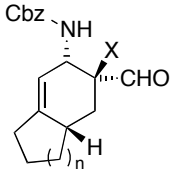 | n = 1, X = Br (**6fa**) | 91 | 80 |
| 13[f] | | n = 2, X = Br (**6ga**) | 98 | 91 |
| 14 | | n = 2, X = Cl (**6gb**) | 76 | 90 |
| 15[d,g] | | n = 3, X = Br (**6ha**) | 85 | 79 |
| 16[f] | 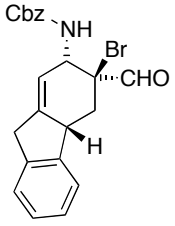 | (**6ia**) | 76 | 87 |
| 17[h,i] | 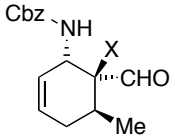 | X = H (**6af**) | 34 | 88 |
| 18[h] | | X = Br (**6ag**) | <1 | — |

[a]Reactions were conducted with 2.0 equiv of **4** and 1.0 equiv of **5** in the presence of 2.5 mol% **2d** in toluene at –60 °C. [b]Isolated yield, see Supporting Information. [c]Determined by chiral HPLC, see Supporting Information. [d]Reactions were conducted with 3.0 equiv of **4** and 1.0 equiv of **5** in the presence of 2.5 mol% **2d** in toluene. [e]Reaction was conducted with 1.0 equiv of **4** and 1.5 equiv of **5e** in the presence of 2.5 mol% **2d** and MS4Å in toluene at –80 °C. [f]Reactions were conducted at –50 °C. [g]*endo* : *exo* = ~5 : 1. [h]Reactions were conducted with 1.0 equiv of **4a** and 12 equiv of **5** in the presence of 5.0 mol% **2d** in toluene. [i]*endo*:*exo* = ~7:1.

**Computational Study by Density Functional Theory (DFT) Calculations for the $C_2$-BISPA 1a-catalyzed Enantioselective Diels–Alder Reaction of Acrolein with *N*-Cbz Amidodiene.** The intriguing behavior of $C_2$- and $C_1$-BISPA catalysts motivated us to study the reaction mechanism in detail. Computational studies were carried out in the following order: (i) the structure of $C_2$-BISPA **1a** was optimized; (ii) the conformations of the amidodienes were optimized, and diastereofacial selection and a simplified transition state (TS) model without any catalyst were investigated; and (iii) a realistic TS model for the $C_2$-BISPA **1a**-catalyzed enantioselective Diels–Alder reaction based on studies (i) and (ii) was explored.[22] All calculations were performed with the Gaussian 09 package.[23] Geometries were fully optimized at the B3LYP/6-31G* level and with ONIOM (B3LYP/6-31G*:HF/3-21G) calculations[24] and characterized by frequency calculations. To evaluate the dispersion interactions such as π-π and CH-π interactions of the Ar groups, single-point energy calculations of the realistic TS models were conducted at the B3LYP-D3/6-31+G** level.[25]

DFT calculations of **1a** showed that the atropo diastereomer (*S*,*R*,*S*) is conformationally more stable than either the (*R*,*R*,*S*) or (*R*,*R*,*R*) diastereomers by 4.2 and 6.7 kcal/mol, respectively. This stability is due to the hydrogen bond between two phosphoric acids (Figure 5). In particular, the hydrogen bond to the phosphoryl oxygen (-O(2)H···O(1)=P) is more stabilizing toward the atropo diastereomeric structure than that toward the ester oxygen (-O(2)H···O(3)-P). This atropo diastereomer (*S*,*R*,*S*) of **1a** is consistent with the X-ray diffraction analysis of $C_2$-BISPA **1b**, which possesses a phenyl group.

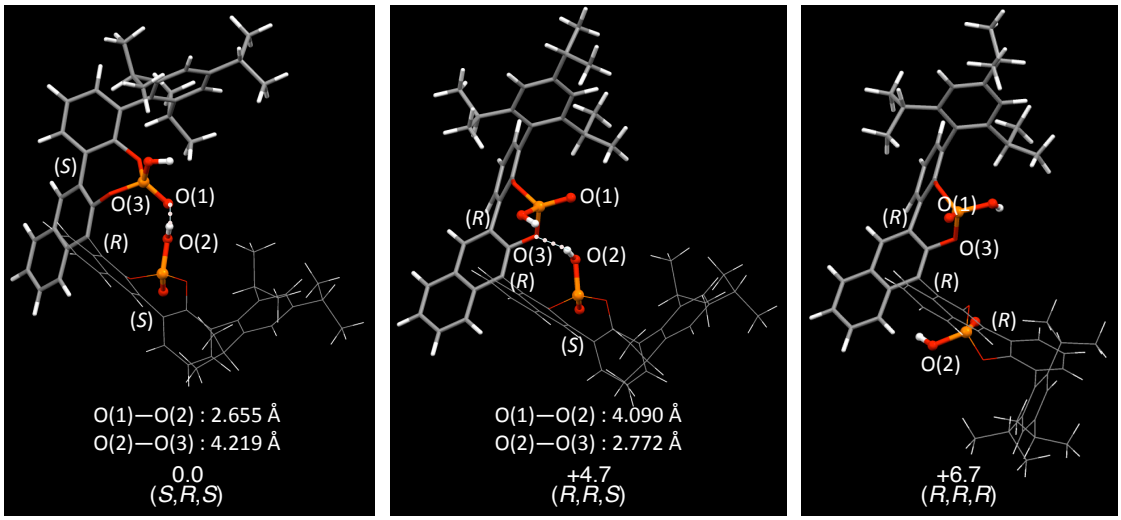


**Figure 5.** Conformational stability of three atropo diastereomers in $C_2$-BISPA **1a**. Hydrogen bonds are indicated by dashed lines. Relative energies (kcal/mol) were calculated based on single-point energy calculation at the B3LYP/6-31G* level.

Based on the optimized catalyst structure of **1a** and the simplified TS model without catalyst, the identified TS models are summarized in Figure 6.[26] To reveal the factors contributing to asymmetric induction, the structural differences between the energetically lowest $\mathbf{TS1}_{\mathbf{1s6r}}$ and $\mathbf{TS1}_{\mathbf{1r6s}}$ structures were investigated. In contrast to the well-established $C_2$-symmetric chiral environment by the mono-phosphoric acid,[27,28] $C_2$-BISPA **1a** provides a distinctive chiral environment due to the presence of a hydrogen-bonding network. In **TS1**, one of the phosphoric acid group acts as a bifunctional catalyst, where the OH group (proton) activates the acrolein and the P=O group accepts the amidodiene with the intervention of hydrogen bonds. A distorted chiral space is formed by one of the phosphoric acid groups activating both the acrolein and the amidodiene. The binaphthyl skeleton of **1a** acts as a linker to position the TRIP group in distorted $C_2$-symmetric fashion. The inter- and intramolecular hydrogen-bonding networks are similar in both $\mathbf{TS1}_{\mathbf{1s6r}}$ and $\mathbf{TS1}_{\mathbf{1r6s}}$. The origin of the energy difference is due to differences in steric repulsion. The benzyl group of the amidodiene is located far from the TRIP group of **1a**, and, thus, there is no unfavorable steric interaction in $\mathbf{TS1}_{\mathbf{1s6r}}$. In contrast, the serious repulsive steric interaction (pink curve in Figure 6) between the benzyl group of amidodiene and the TRIP group of **1a** is responsible for the destabilization of $\mathbf{TS1}_{\mathbf{1r6s}}$.[29]

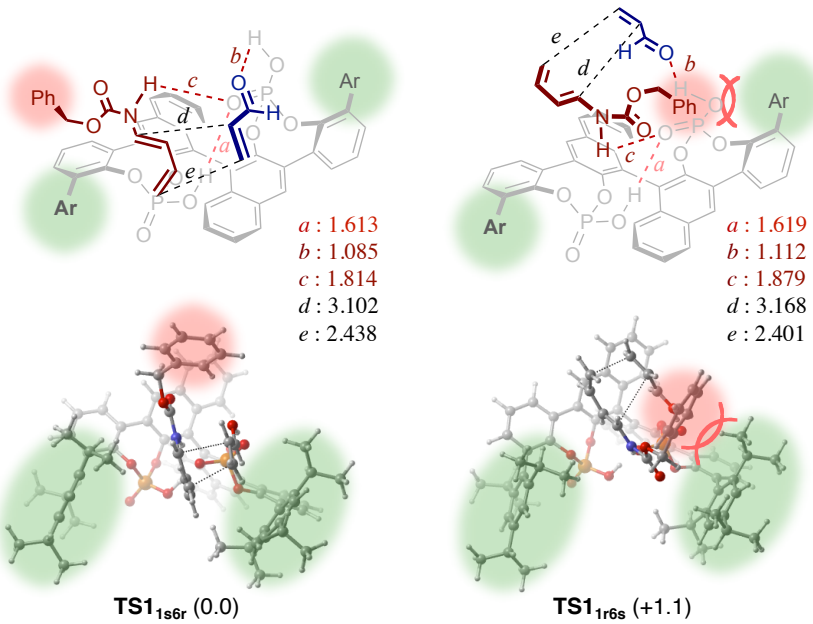


**Figure 6.** 3D structures, schematic representation models, and relative energies (kcal/mol) of **TS1**$_{1s6r}$ and **TS1**$_{1r6s}$. Bond lengths are shown in Å.

**DFT Calculations of $C_1$-BISPA 2d-catalyzed Enantioselective Diels–Alder Reaction of Acrolein 5d with *N*-Cbz Amidodiene 4a.** To reveal the influence of the electron-withdrawing groups in the $C_1$-symmetric design in more detail, theoretical investigations of the TS models were conducted for the $C_1$-BISPA **2d**-catalyzed reaction of acrolein **5d** with amidodiene **4a** (Table 3, entry 4: 98% ee) based on the DFT calculations for $C_2$-BISPA **1a**. There are two possible coordination sites on the phosphoric acid units, one close to the TRIP group (**TS2a**) and the other close to the $C_6F_5$ group (**TS2b**). The different chiral spaces are modified both sterically and electronically, allowing fine tuning of chiral spaces in $C_1$-BISPA **2d**. The chiral spaces lead to major and minor enantiomers *via* transition states **TS2**$_{1s6r}$ and **TS2**$_{1r6s}$. Therefore, four diastereomeric **TS2** models were compared to establish the optimal $C_1$-symmetric catalyst design (Figure 7).[30]

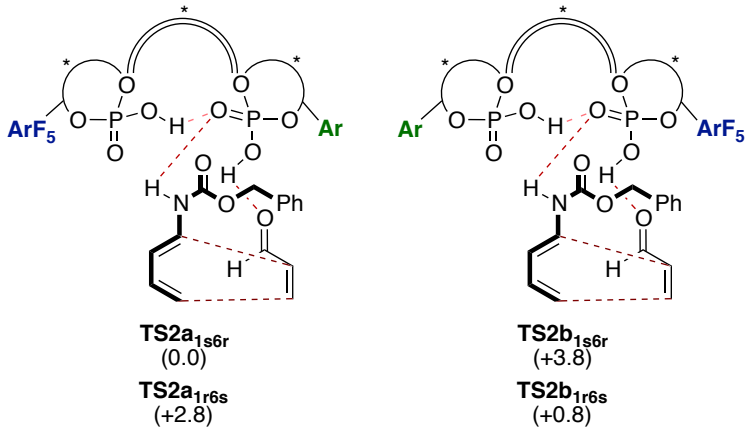


**Figure 7**. Two possible coordination sites, and the relative energies (kcal/mol) of four diastereomeric **TS2** models.

Each favorable TS model that we identified for both major and minor enantiomers is summarized in Figure 8. The chiral space in **TS2a**$_{1s6r}$ is smaller than that in **TS2b**$_{1r6s}$, and the intramolecular hydrogen bond between the two phosphoric acid units becomes shorter in **TS2a**$_{1s6r}$ (1.587 Å) than in **TS2b**$_{1r6s}$ (1.632 Å) due to the increased acidity of the bridged phosphoric acid close to the $C_6F_5$ group. A comparison of the favorable TS models for major and minor enantiomers shows that **TS2a**$_{1s6r}$ is more stable than **TS2b**$_{1r6s}$ by 0.8 kcal/mol. We believe that the energy differences arise from the inherent conformational stability of the catalyst structure and from the steric repulsion between the benzyl group of amidodiene **5a** and the $C_6F_5$ group of **2d**. In fact, as we reported previously, 99% ee was obtained in the reaction catalyzed by the $C_2$-BISPA catalyst **1a** that has a TRIP substituent. In contrast, the enantioselectivity dropped in the reaction catalyzed by $C_2$-BISPA **1d**, which has $C_6F_5$ substituents (60% ee), corroborating our hypothesis that the highly enantioselective reaction by $C_1$-BISPA **2d** (98% ee) preferentially occurs on the side of the catalyst nearest the TRIP substituent and between the two asymmetric reaction spaces in $C_1$-BISPA **2d**. This differentiation of the asymmetric reaction space created by the electronic effects is an important feature of our catalyst design.

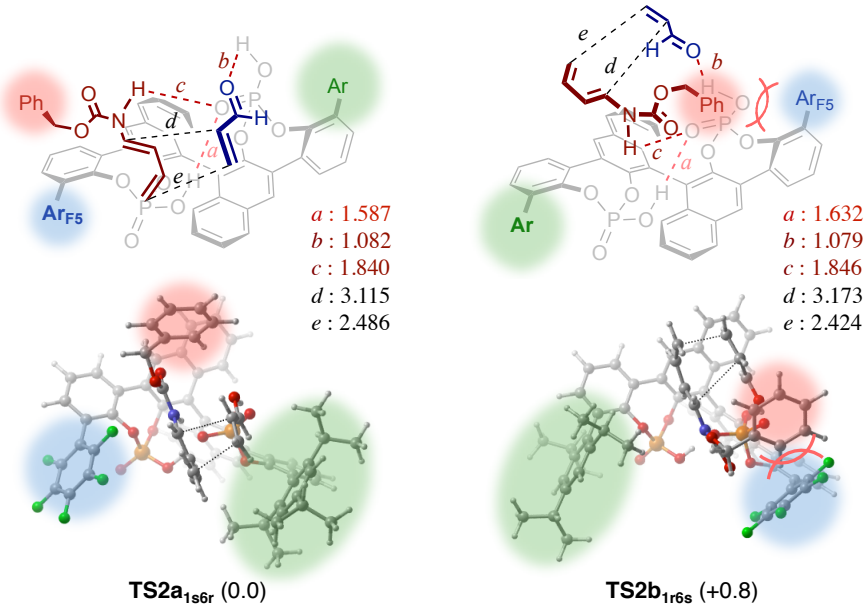


**Figure 8**. 3D structures, schematic representations, and relative energies (kcal/mol) in **TS2**. Bond lengths are shown in Å.

## ■ CONCLUSION

In summary, we have successfully developed the $C_1$-BISPA **2d** catalyst that possesses both TRIP and $C_6F_5$ groups, which efficiently catalyzed the highly diastereo- and enantioselective Diels–Alder reactions of acrolein, methacrolein, and α-haloacroleins with amidodienes. Furthermore, we have conducted DFT calculations for TS models of the $C_2$-BISPA **1a** and $C_1$-BISPA **2d**-catalyzed enantioselective Diels–Alder reaction of acrolein with amidodiene. We have confirmed that intramolecular hydrogen bonding between the phosphoric acid proton and phosphoryl oxygen ($-OH_{C6F5}\cdots O{=}P_{TRIP}$) plays an important role in creating the $C_1$-symmetric chiral environment, in which high enantioselectivities and yields were realized. The asymmetric reaction space could be elaborated by the electronic and steric effects of the naphthyl—*ortho*-biphenyl framework at the side of the $C_{Naph}(1')—C_{Naph}(3')$-$C_{Ar}(3)$ position. The catalytic activity was adequately provided by the electron-withdrawing $C_6F_5$ group to improve the chemical yields of the Diels–Alder products. This design concept based on a $C_1$-symmetric framework has great potential and is broadly applicable to the development of other chiral Brønsted acid catalysts. Further studies on this are underway in our laboratories and will be reported in due course.

## ■ ASSOCIATED CONTENT

The Supporting Information Available:

Experimental details, characterization data, HPLC enantiomer analysis, NMR spectra for new compounds, X-ray diffraction analysis, and description of mechanistic features, structural details of the transition states, and Cartesian coordinates (PDF).

15 KF C1-BISPA ACS Catalysis 150918 SI cif C1BISPA(CF3)2C6H3 2b (CIF)

15 KF C1-BISPA ACS Catalysis 150918 SI cif OMe protected CMPA 3b (CIF)

This material is available free of charge via the Internet at http://pub.acs.org.

## ■ AUTHOR INFORMATION

**Corresponding Authors**

*E-mail: momiyama@ims.ac.jp

*E-mail: mterada@m.tohoku.ac.jp

**Notes**

The authors declare no competing financial interest.

## ■ ACKNOWLEDGMENTS

Support was partially provided by JSPS via Grant-in-Aid for Scientific Research C (No. 23550114), and Grant-in-Aid for Scientific Research on Innovative Areas “Advanced Molecular Transformations by Organocatalysts” from MEXT, Japan (No. 23105002, No. 23105005). We thank Prof. Yasuhiro Uozumi (Institute for Molecular Science) and Associate Prof. Souji Shimizu (Graduate School of Engineering, Kyushu University) for helpful discussion. We also thank the Yoshida Scholarship Foundation (K. F.).

## ■ REFERENCES

(1) (a) Noyori, R. *Asymmetric Catalysis in Organic Synthesis*; Wiley: New York, 1994. (b) *Comprehensive Asymmetric Catalysis*; Jacobsen, E. N., Pfaltz, A., Yamamoto, H., Eds.; Springer: Berlin, 1999. (c) *Catalytic Asymmetric Synthesis*, 3rd ed.; Ojima, I., Ed.; Wiley-VCH: New York, 2010.

(2) (a) Yoon, T. P.; Jacobsen, E. N. *Science* **2003**, *299*, 1691-1693. (b) *Privileged Chiral Ligands and Catalysts*; Zhou, Q.-L., Ed.; Wiley-VCH: Weinheim, 2011.

(3) For selected reviews, see: (a) Brunel, J. M. *Chem. Rev.* **2005**, *105*, 857-897. (b) Akiyama, T. *Chem. Rev.* **2007**, *107*, 5744-5758. (c) Shibasaki, M.; Kanai, M.; Matsunaga, S.; Kumagai, N. *Acc. Chem. Res.* **2009**, *42*, 1117-1127. (d) Hatano, M.; Ishihara, K. *Synthesis* **2010**, 3785-3801. (e) Pereira, M. M.; Abreu, A. R.; Calvete, M. J. F.; Carrilho, R. M. B. *Adv. Chem. Res.* **2013**, *19*, 111-153.

(4) (a) Momiyama, N.; Konno, T.; Furiya, Y.; Iwamoto, T.; Terada, M. *J. Am. Chem. Soc.* **2011**, *133*, 19294-19297. (b) Hong, L.; Kai, M.; Wu, C.; Sun, W.; Zhu, G.; Li, G.; Yao, X.; Wang, R. *Chem. Commun.* **2013**, *49*, 6713-6715.

(5) For linked BINOL-derived chiral bis-phosphoric acid catalyst, see: (a) Chen, X. H.; Zhang, W. Q.; Gong, L. Z. *J. Am. Chem. Soc.* **2008**, *130*, 5652-5653. (b) Yu, J.; He, L.; Chen, X. H.; Song, J.; Chen, W. J.; Gong, L. Z. *Org. Lett.* **2009**, *11*, 4946-4949. (c) Yu, J.; Chen, W. J.; Gong, L. Z. *Org. Lett.* **2010**, *12*, 4050-4053. (d) He, L.; Chen, X. H.; Wang, D.; Luo, S. W.; Zhang, W. Q.; Yu, J.; Ren, L.; Gong, L. Z. *J. Am. Chem. Soc.* **2011**, *133*, 13504-13518. (e) Guo, C.; Song, J.; Gong, L. *Org. Lett.* **2013**, *15*, 2676-2679.

(6) For related studies, see: (a) Inanaga, J. *Organomet. News* **2008**, 20-24. (b) Inanaga, J. *Fain Chemical* **2008**, *37*, 33-40.

(7) Wolf, C. *Dynamic Stereochemistry of Chiral Compounds*; RSC Publishing: Cambridge, 2008.

(8) For selected reviews on the use of conformationally flexible achiral and meso biaryl ligands in transition metal catalyzed asymmetric synthesis, see: (a) Walsh, P. J.; Lurain, A. E.; Balsells, J. *Chem. Rev.* **2003**, *103*, 3297-3344. (b) Mikami, K.; Yamanaka, M. *Chem. Rev.* **2003**, *103*, 3369-3400. (c) Reetz, M. T. *Angew. Chem., Int. Ed.* **2008**, *47*, 2556-2588. (d) Aikawa, K., Mikami, K. *Chem. Commun.* **2012**, *48*, 11050-11069.

(9) For impressive reports on the use of an achiral, conformationally flexible biphenyl subunit for the molecular design of chiral organocatalyst, see: (a) Ooi, T.; Uematsu, Y.; Kameda, M.; Maruoka, K. *Angew. Chem., Int. Ed.* **2002**, *41*, 1551-1554. (b) Matsui, K.;

Takizawa, S.; Sasai, S. *Synlett* **2006**, 761-765.

(10) For reviews of hydrogen bonding, see: (a) Seebach, D.; Beck, A.; Heckel, K. *Angew. Chem., Int. Ed.* **2001**, *40*, 92-138. (b) Steiner, T. *Angew. Chem., Int. Ed.* **2002**, *41,* 48-76.

(11) For optically active BINOL-derived $C_1$-symmetric catalyst, see: (a) Amano, M.; Watanabe, M.; Baba, N.; Oda, J.; Inouye, Y. *Bull. Chem. Soc. Jpn.* **1983**, *56*, 3672-3678. (b) Uraguchi, D.; Koshimoto, K.; Ooi, T. *Chem. Commun.* **2010**, *46*, 300-302. (c) Uraguchi, D.; Koshimoto, K.; Sanada, C.; Ooi, T. *Tetrahedron: Asymmetry* **2010**, *21*, 1189-1190.

(12) For selected examples of catalytic enantioselective Diels–Alder reaction of α-haloacrolein, see: (a) Corey, E. J.; Loh, T.-P. *J. Am. Chem. Soc.* **1991**, *113*, 8966-8967. (b) Corey, E. J.; Loh, T.-P. *Tetrahedron Lett.* **1993**, *34*, 3979-3982. (c) Hatano, M.; Mizuno, T.; Izumiseki, A.; Usami, R.; Asai, T.; Akakura, M.; Ishihara, K. *Angew. Chem., Int. Ed.* **2011**, *50*, 12189-12192.

(13) For selected examples of enantioselective reaction using amino dienes, see: (b) Huang, Y.; Iwama, T.; Rawal, V. H. *J. Am. Chem. Soc.* **2000**, *122*, 7843-7844. (c) Huang, Y.; Iwama, T.; Rawal, V. H. *J. Am. Chem. Soc.* **2002**, *124*, 5950-5951. (d) Huang, Y.; Iwama, T.; Rawal, V. H. *Org. Lett.* **2002**, *4*, 1163-1166. (e) Tian, X.; Hofman, N.; Melchiorre, P. *Angew. Chem., Int. Ed.* **2014**, *53*, 2997-3000. (f) Kong, L.; Han, X.; Jiao, P. *Chem. Commun.* **2014**, *50*, 14113-14116. (g) Pous, J.; Courant, T.; Bernadat, G.; Iorga, B. I.; Blanchard, F.; Masson, G. *J. Am. Chem. Soc.* **2015**, *137*, 11950-11953.

(14) (a) Overman, L. E.; Taylor, G. F.; Petty, C. B.; Jessup, P. J. *J. Org. Chem.* **1978**, *43*, 2164-2167. (b) Overman, L. E.; Jessup, P. J. *J. Am. Chem. Soc.* **1978**, *100*, 5179-5185.

(15) (a) Wipf, P.; Wang, X. *Tetrahedron Lett.* **2000**, *41*, 8747-8751. (b) Huang, J.; Bergmeier, S. C. *Tetrahedron* **2008**, *64*, 6434-6439.

(16) Selected examples of chiral Brønsted acid catalyzed enantioselective Diels–Alder reaction of α,β-unsaturated carbonyl compounds with dienes, see: (a) Nakashima, D.; Yamamoto, H. *J. Am. Chem. Soc.* **2006**, *128*, 9626-9627. (b) Borovia, A.; Nagorny, P. *Tetrahedron* **2013**, *69*, 5719-5725. (c) Tian, X.; Hofmann, N.; Melchiorre, P. *Angew. Chem., Int. Ed.* **2014**, *53*, 2997-3000.

(17) X-ray diffraction analysis of **3b** was shown in Supporting Information.

(18) Details for X-ray diffraction analysis of **2b** were shown in Supporting Information.

(19) Details for the reactions of α-haloacroleins were provided in Supporting Information.

(20) For selected examples, see: (a) Huang, Y.; Unni, A. K.; Thadani, A. N.; Rawal, V. H. *Nature* **2003**, *424*, 146. (c) Thadani, A. N.; Stankovic, A. R.; Rawal, V. H. *Proc. Natl. Acad. Sci. U.S.A.* **2004**, *101*, 5846-5850. (d) Unni, A. K.; Takenaka, N.; Yamamoto, H.; Rawal, V. H. *J. Am. Chem. Soc.* **2005**, *127*, 1336-1337. (e) Momiyama, N.; Yamamoto, H. *J. Am. Chem. Soc.* **2005**, *127*, 1080-1081. (f) Hasegawa, A.; Naganawa, Y.; Fushimi, M.; Ishihara, K.; Yamamoto, H. *Org. Lett.* **2006**, *8*, 3175-3178. (g) Hashimoto, T.; Maruoka, K. *J. Am. Chem. Soc.* **2007**, *129*, 10054-10055. (h) Hashimoto, T.; Kimura, H.; Nakatsu, H.; Maruoka, K. *J. Org. Chem.* **2011**, *76*, 6030-6037. (i) Ratjen, L.; Gemmeren, M.; Pesciaioli, F.; List, B. *Angew. Chem., Int. Ed.* **2014**, *53,* 8765-8769.

(21) (a) Overman, L. E.; Jessup, P. J. *Tetrahedron Lett.* **1977**, *18*, 1253-1256. (b) Overman, L. E.; Jessup, P. J. *J. Am. Chem. Soc.* **1978**, *100*, 5180-5185. (c) Masamune, S.; Reed, L. A.; Davis, J. T.; Choy, W. *J. Org. Chem.* **1983**, *48*, 4441-4444.

(22) Details were provided in Supporting Information.

(23) Frisch, M. J.; Trucks, G. W.; Schlegel, H. B.; Scuseria, G. E.; Robb, M. A.; Cheeseman, J. R. Scalmani, G.; Barone, V.; Mennucci, B.; Petersson, G. A.; Nakatsuji, H.; Caricato, M.; Li, X.; Hratchian, H. P.; Izmaylov, A. F.; Bloino, J.; Zheng, G.;

Sonnenberg, J. L.; Hada, M.; Ehara, M.; Toyota, K.; Fukuda, R.; Hasegawa, J.; Ishida, M.; Nakajima, T.; Honda, Y.; Kitao, O.; Nakai, H.; Vreven, T.; Montgomery, Jr., J. A.; Peralta, J. E.; Ogliaro, F.; Bearpark, M.; Heyd, J. J.; Brothers, E.; Kudin, K. N.; Staroverov, V. N.; Keith, T.; Kobayashi, R.; Normand, J.; Raghavachari, K.; Rendell, A.; Burant, J. C.; Iyengar, S. S.; Tomasi, J.; Cossi, M.; Rega, N.; Millam, J. M.; Klene, M.; Knox, J. E.; Cross, J. B.; Bakken, V.; Adamo, C.; Jaramillo, J.; Gomperts, R.; Stratmann, R. E.; Yazyev, O.; Austin, A. J.; Cammi, R.; Pomelli, C.; Ochterski, J. W.; Martin, R. L.; Morokuma, K.; Zakrzewski, V. G.; Voth, G. A.; Salvador, P.; Dannenberg, J. J.; Dapprich, S.; Daniels, A. D.; Farkas, O.; Foresman, J. B.; Ortiz, J. V.; Cioslowski, J.; Fox, D. J. Gaussian09, Revision D.01; Gaussian, Inc.: Wallingford, CT, 2013.

(24) For selected examples, see: (a) Dapprich, S.; Komaromi, I.; Byun, K. S.; Morokuma, K.; Frisch, M. J. *J. Mol. Struct. (THEOCHEM)* **1999**, *461-462*, 1-21. (b) Svensson, M.; Humbel, S.; Morokuma, K. *J. Chem. Phys.* **1996**, *105*, 3654-3661. (c) Vreven, T; Morokuma, K. *J. Comput. Chem.* **2000**, *21*, 1419-1432.

(25) Grimme, S.; Antony, J.; Ehrlich, S.; Krieg, H. *J. Chem. Phys.* **2010**, *132*, 154104.

(26) Details were provided in Supporting Information.

(27) Seminal study, see: (a) Akiyama, T.; Itoh, J.; Yokota, K.; Fuchibe, K. *Angew. Chem., Int. Ed.* **2004**, *43*, 1566-1568. (b) Uraguchi, D.; Terada, M. *J. Am. Chem. Soc.* **2004**, *126*, 5356-5357. (c) Terada, M.; Kanomata, K. *Synlett* **2011**, 1255-1258.

(28) For recent reviews, see: (a) Akiyama, T. In S*cience of Synthesis, Asymmetric Organocatalysis 2*, *Brønsted Base and Acid Catalysts, and Additional Topics*, Maruoka, K. Ed.; Georg Thieme Verlag KG: New York, 2012; Vol. 2, pp 169-217. (b) Terada, M.; Momiyama, N.; In *Science of Synthesis, Asymmetric Organocatalysis 2, Brønsted Base and Acid Catalysts, and Additional Topics*, Maruoka, K. Ed.; Georg Thieme Verlag KG: New York, 2012; Vol. 2, pp 219-296. (c) Parmar, D.; Sugiono, E.; Raja, S.; Rueping, M.; *Chem. Rev.* **2014**, *114*, 9047-9153.

(29) Although the benzyl group is freely rotating, there is still significant steric repulsion caused by two TRIP groups. The other TS model obtained by rotation of the benzyl group toward the opposite side of the TRIP group is 2.7 kcal/mol less stable than **TS1**$_{\mathbf{1r6s}}$.

(30) Details were shown in Supporting Information.